Inorganica Chimica Acta 363 (2010) 1869–1878

Contents lists available at ScienceDirect

Inorganica Chimica Acta

journal homepage: www.elsevier.com/locate/ica

Synthesis and investigation of spectral and electrochemical properties of alkyl-substituted planar binuclear phthalocyanine complexes sharing a common naphthalene ring

Tatiana V. Dubinina [a,b,*], Aleksey V. Ivanov [b], Natalia E. Borisova [a], Stanislav A. Trashin [b], Stanislav I. Gurskiy [a], Larisa G. Tomilova [a,b], Nikolay S. Zefirov [a]

[a] Chemistry Department, M.V. Lomonosov Moscow State University, 1 Leninskie Gory, 119991 Moscow, Russia
[b] Institute of Physiologically Active Compounds, 1 Severny Proezd, 142432 Chernogolovka, Moscow Region, Russia

ARTICLE INFO

Article history:
Received 23 December 2009
Received in revised form 8 February 2010
Accepted 11 February 2010
Available online 16 February 2010

Keywords:
Binuclear phthalocyanines
UV/Vis spectroscopy
Fluorescence spectroscopy
Voltammetry
Spectroelectrochemistry

ABSTRACT

Hexa-*tert*-butyl and dodeca-*n*-butyl-substituted planar binuclear phthalocyanines sharing a common naphthalene ring with Mg as a central metal were synthesized with high yields and characterized by UV/Vis spectra, luminescence spectra, NMR, electrochemical, and spectroelectrochemical measurements. On the base of these complexes, the metal-free phthalocyanine ligands and the series of binuclear phthalocyanine complexes of rare earth elements (REE) were synthesized.

All compounds obtained revealed an intensive near IR-absorption reaching 855 nm for trinuclear phthalocyanine. A crucial increase in NMR spectra resolution was achieved by the addition of ethylene glycol as a disaggregating agent. Spectroelectrochemical measurements during oxidation showed reversible changes of absorbance at 709 and 800 nm.

1. Introduction

The use of phthalocyanines in numerous applications has expanded rapidly [1–4] in the last decade. This has inspired investigators to synthesize new analogues and then to determine the "structure–properties" correlationship, and novel compounds with modulated properties have also been obtained.

Planar binuclear phthalocyanines are of increasing importance due to their potential use in non-linear optical [1] and data storage devices, and as laser dyes [5]. In previous work [6] we have reported intensive absorption in the near IR-region and 200 nm red shift of the Q-band for planar binuclear phthalocyanines sharing a common benzene ring compared with corresponding monophthalocyanines. These peculiarities are due to the extended aromatic system and allow the use of planar binuclear phthalocyanines as effective solid and liquid phase colour filters as well as IR-labels.

The first attempt to increase the aromatic bridge from benzene to naphthalene was realized by Yang et al. [5]. However, the target compound was obtained in only 6% yield, while absorption in the near IR-region was not revealed. In subsequent researches no significant progress was achieved in this area [1,7]. Thus, the data obtained for this type of binuclear phthalocyanine are unclear and contradictory [1,5,7]. Moreover, to our knowledge, no electrochemical and spectroelectrochemical investigations have been performed for planar binuclear phthalocyanines sharing a common naphthalene ring, although such data were obtained in the case of analogues with a common benzene ring [8,9].

The main purpose of the current work was the synthesis of new alkyl-substituted planar binuclear phthalocyanines sharing a common naphthalene ring and investigation of their properties.

2. Experimental

UV/Vis spectra were recorded using a Helios-α spectrophotometer in quartz cells (0.5 × 1 cm) using pyridine, DMSO, CH_3CN, C_6H_6, and THF as solvents. The fluorescence spectra were recorded on a Perkin–Elmer LS 55 (xenon discharge lamp, $U = 775$ V) spectrometer in quartz cells (1 × 1 cm). ^1H and ^{13}C NMR spectra were recorded on a Bruker "Avance 400" spectrometer (400.13 and 100.61 MHz, respectively) using $CDCl_3$, DMSO-d_6, and Py-d_5 as solvents at 20 °C (if not additionally specified). Chemical shifts are given in ppm relative to $SiMe_4$. Coupling constants, J, are given in Hz. The column chromatography was performed using Lancaster Silica Gel 60 (0.060–0.200 mm) and Merck Silica Gel 40 (0.063–0.200 mm). Preparative TLC was performed using flexible plates Merck Silica Gel 60 F_{254} and Merck Aluminium Oxide F_{254} neutral.

* Corresponding author. Address: Chemistry Department, M.V. Lomonosov Moscow State University, 1 Leninskie Gory, 119991 Moscow, Russia. Tel.: +7 495 939 1243; fax: +7 495 939 0290.
E-mail addresses: dubinina.t.vid@gmail.com (T.V. Dubinina), tom@org.chem.msu.ru (L.G. Tomilova).

0020-1693/$ - see front matter © 2010 Elsevier B.V. All rights reserved.
doi:10.1016/j.ica.2010.02.011

The gel permeation chromatography was performed using Bio Beads SX-1 (Bio Rad). The CHN analysis was carried out using a CHNOS Elemental Analyzer vario MICRO. Mass-spectra were recorded on a Finnigan MAT INSOC-50 (EI 70 eV) and a VISION-2000 (MALDI-TOF). IR-spectra were recorded on a spectrophotometer SPECORD M-70 и SPECORD UR-20 in liquid paraffin and using KBr discs.

The salts, $Mg(OAc)_2{\cdot}4H_2O$, $Ni(OAc)_2{\cdot}4H_2O$, $Lu(OAc)_3{\cdot}4H_2O$, $Er(OAc)_3{\cdot}4H_2O$, and $Gd(OAc)_3{\cdot}3H_2O$, were dried under vacuum at 100 °C for 4 h immediately before use. 4,5-Dibutyl-phthalonitrile [10] and 4-*tert*-butyl-phthalonitrile [11] were synthesized according to the published procedures. The magnesium complex of 2(3),9(10),16(17),23(24)-tetra-*tert*-butylphthalocyanine (*t*BuPcMg) was obtained as a by-product of **6a** synthesis and was separated by gel permeation chromatography.

Electrochemical measurements were carried out with an IPC-Pro potentiostat (Econix, Moscow, Russia). Cyclic voltammetry was performed in a conventional three electrode cell using Pt-disk (2.0 mm in diameter) working and Pt-foil counter electrodes. The Ag|AgCl reference electrode was connected to the solution through a salt-bridge and a Luggin capillary, whose tip was placed close to the working electrode. The junction potentials were corrected by ferrocenium$^+$/ferrocene (Fc^+/Fc) couple. 0.1 mol/l solution of Bu_4NBF_4 (Sigma–Aldrich, recrystallized and dried under vacuum at +70 °C) in o-dichlorobenzene (DCB, 99% Sigma–Aldrich, HPLC-grade) containing 1–5 $\times$ 10^{-4} M of sample was bubbled with argon for 20 min before measurements were taken.

Spectroelectrochemical experiments were performed with a quartz electrochemical cell composed of three separated compartments. The 9.3 mm path-length rectangular compartment contained a Pt-net working electrode, which was placed near the sidewall to avoid an influence on the light beam. A Luggin capillary and a capillary for argon bubbling were close to the working electrode. A reference Ag|AgCl electrode was connected to the cell through a salt-bridge. A Pt-counter electrode with a surface area larger than the area of the working electrode was in a separate compartment connected to the working space through a glass tube with a frit. Pure argon was used to remove oxygen from sample solutions and for gentle stirring during the electrolysis. To measure equilibrium potentials at different stages of electrolysis, the open circuit potential was recorded until a stable value was reached.

2.1. Synthesis of isoindolo[5,6-f]isoindole-1,3,6,8(2H,7H)-tetraimine

2.1.1. 1,2-Dibromo-4,5-bis(dibromomethyl)benzene **2**

1,2-Dibromo-4,5-dimethylbenzene (6.60 g, 25.00 mmol) was dissolved in CCl_4 (38 mL) under reflux. Bromine (5 mL, 0.1 mol) was then slowly added dropwise to the stirring solution under irradiation with a 300 W lamp for 7 h (TLC-control: silica gel, *n*-hexane). The reaction mixture was cooled to room temperature and washed by an aqueous solution of $Na_2S_2O_3$. The organic layer was dried with $CaCl_2$. The solvent was evaporated and the resulting solid was recrystallized from *n*-hexane: ethyl acetate (1:1 V/V) to give white crystals of **2** (9.74 g, 67%), m.p. 131.8 (lit. 132 °C [12]), R_f = 0.38 (silica gel, *n*-hexane).

2.1.2. 6,7-Dibromonaphthalene-2,3-dicarbonitrile **3**

1,2-Dibromo-4,5-bis(dibromomethyl)benzene **2** (16.68 g, 29.00 mmol), fumaronitrile (3.40 g, 44.00 mmol) and sodium iodide (14.0 g, 93.00 mmol) was stirred in DMF (153 mL) at 70 °C for 4.5 h (TLC-control: Al_2O_3, C_6H_6). The reaction mixture was cooled to room temperature and water was added. The product was collected by filtration and washed by aqueous solution of $Na_2S_2O_3$. Then the precipitate was recrystallized from CCl_4. Additional purification was carried out using sublimation (290 °C, p = 10 mm Hg). Complex **3** was obtained as white crystals (8.69 g, 89%), m.p. 317 °C (in the sealed capillary), R_f = 0.51 (Al_2O_3, C_6H_6). ^{1}H NMR (400.13 MHz, $CDCl_3$, 20 °C): δ = 8.24 (s, 2H, H_{Ar} – 1, 4); 8.29 (s, 2H, H_{Ar} – 5, 8). ^{13}C NMR (100.61 MHz, $(CD_3)_2SO$, 20 °C): δ = 110.10 (s, C2, C3); 116.04 (s, CN); 126.86 (s, C6, C7); 132.37 (s, C9, C10); 133.17 (s, C1, C4); 135.57 (s, C5, C8). *Anal.* Calc. for $C_{12}H_4Br_2N_2$: C, 42.90; H, 1.20; N, 8.34. Found: C, 42.77, 42.66; H, 1.25; 1.38; N, 8.11, 8.12%.

2.1.3. Naphthalene-2,3,6,7-tetracarbonitrile **4**

6,7-Dibromonaphthalene-2,3-dicarbonitrile **3** (2.23 g, 6.60 mmol) and CuCN (2.98 g, 33.00 mmol) were stirred in DMF (45 mL) under reflux in the flux of argon for 5 h (TLC-control: Al_2O_3, C_6H_6:CH_3CN (10:1 V/V)). The reaction mixture was cooled to room temperature and the saturated aqueous solution of $FeCl_3{\cdot}6H_2O$ was added. The black precipitate was filtered and washed with NH_3aq. Then the precipitate was dissolved in CH_3CN and heated to reflux. The insoluble admixtures were filtered. The filtrate was evaporated and the resulting solid was additionally purified using column chromatography (SiO_2, acetone: C_6H_6 (1:15 V/V)) to give **4** (1.028 g, 68%), R_f = 0.70 (Al_2O_3, C_6H_6:CH_3CN (10:1 V/V)). The compound is decomposed under melting (360 °C). ^{1}H NMR (400.13 MHz, $(CD_3)_2SO$, 20 °C): δ = 9.01 (s, 4H, H_{Ar} – 1, 4, 5, 8). IR (liquid paraffin): ν_{max}/cm^{-1} 2255 ($\nu_{C\equiv N}$). MS (EI) m/z: 228 (M^+). *Anal.* Calc. for $C_{14}H_4N_4$: C, 73.68; H, 1.77; N, 24.55. Found: C, 73.77, 73.44; H, 1.88, 1.75; N, 24.05, 24.67%.

2.1.4. Isoindolo[5,6-f]isoindole-1,3,6,8(2H,7H)-tetraimine **5**

Naphthalene-2,3,6,7-tetracarbonitrile **4** (100 mg, 0.40 mmol) was stirred in MeONa–MeOH solution (7.0 mg Na in 10 mL MeOH) under cooling for 4 h with dry NH_3 bubbled through the solution (TLC-control: Al_2O_3, C_6H_6:CH_3CN (10:1 V/V)). The IR-spectrum of the target compound did not exhibit nitrile absorption observed for the starting nitrile at 2255 cm^{-1} ($\nu_{C\equiv N}$). The brown precipitate was filtered and washed by MeOH and Et_2O to give **5** (80 mg, 70%), R_f = 0 (Al_2O_3, F_{254}, C_6H_6:CH_3CN (10:1 V/V)). IR (liquid paraffin): ν_{max}/cm^{-1} 1650 ($\nu_{C=N}$), 1210–1030 ($\nu_{C-H,\ Ar}$), 735 (ν_{N-H}).

2.2. Synthesis of binuclear phthalocyanine complexes

2.2.1. Reaction in DMAE

*2.2.1.1. (Bis(9(10)^2,14(15)^2,19(20)^2-tri-tert-butyltribenzo [i,n,s]-7,12,17,22-tetraazaporphyrino)[b,g] naphthalene) dimagnesium **6a**.* The mixture of **5** (64 mg, 0.30 mmol), 4-*tert*-butylphthalonitrile (920 mg, 5.00 mmol), and $Mg(OAc)_2{\cdot}4H_2O$ (180 mg, 0.80 mmol) in DMAE (10 mL) was heated to reflux under argon for 17 h. The reaction mixture was cooled to room temperature and the mixture MeOH:H_2O (1:1 V/V) was added. The blue precipitate was filtered and washed by water and MeOH. The target compound **6a** (19 mg, 6%) was separated using gel permeation chromatography (C_6H_6). ^{1}H NMR (400.13 MHz, Py:$CDCl_3$ (1:7 V/V), 20 °C): δ = 1.95–2.19 (m, 54H, H^t_{Bu}); 8.29–8.55, 9.45–10.03 (m, H_{Ar}); 10.56–11.03 (br s, H_{Nph}). MS (MALDI-TOF), m/z: 1381 $[M]^+$, 2763 2·$[M]^+$, 4144 3·$[M]^+$. UV/Vis (THF) λ_{max}/nm (log ε): 358 (5.13); 709 (5.06); 743 (5.12); 789 (5.52). IR (KBr): ν_{max}/cm^{-1} 3081, 3058, 3024 (ν_{C-H}); 1582, 1600 ($\nu_{C=N}$); 1392, 1362 (ratio of intensity 1:2, $\nu_{C(CH3)3}$).

The 2(3),9(10),16(17)-tri-*tert*-butyl-25,26-dicyano-phthalocyanine magnesium **8** (20 mg, 10%) was separated using column chromatography (Al_2O_3, $CHCl_3$: EtOH (100:1 V/V)), and then additionally purified using gel permeation chromatography (C_6H_6). MS (MALDI-TOF), m/z: 823 $[M]^+$, 810 $[M-Me]^+$, 795 $[M-2Me]^+$. UV/Vis (THF) λ_{max}/nm: 355, 634, 674, 700.

2.2.2. Reaction in i-AmOH

*2.2.2.1. (Bis(9(10)^2,14(15)^2,19(20)^2-tri-tert-butyltribenzo [i,n,s]-7,12,17,22-tetraazaporphyrino)[b,g] naphthalene) dimagnesium **6a**.* A mixture of **5** (48 mg, 0.18 mmol), 4-*tert*-butylphthalonitrile

(673 mg, 4.00 mmol), and $Mg(OAc)_2{\cdot}4H_2O$ (157 mg, 0.73 mmol) in *i*-AmOH (12 mL) in the presence of DBU (0.5 mL) was heated to reflux under argon for 8 h. The reaction mixture was cooled to room temperature and the mixture MeOH:H_2O (1:1 V/V) was added. The blue precipitate was filtered and washed by water and MeOH. The target compound **6a** (49 mg, 19.5%) was separated using gel permeation chromatography (C_6H_6). The characteristics of the compound obtained were identical with those obtained by method *a*.

The trinuclear magnesium complex **9** (29 mg, 8%) was separated using gel permeation chromatography. ^1H NMR (400.13 MHz, Py: MeOD (40:1 V/V), 20 °C): δ = 0.87–2.22 (m, 72H, H^t_{Bu}); 6.57–6.88 (m, 24H, H_{Ar}); 7.27–7.44 (m, 8H, H_{Nph}). MS (MALDI-TOF), *m*/*z*: 2003 $[M]^+$. UV/Vis (THF) λ_{max}/nm: 356; 809; 832; 855.

2.2.3. (Bis(9²,10²,14²,15²,19²,20²-hexa-butyltribenzo [i,n,s]-7,12,17,22-tetraazaporphyrino)[b,g] naphthalene) dimagnesium ***6b***

The mixture of **5** (16 mg, 0.040 mmol), 4-*tert*-butylphthalonitrile (240 mg, 0.83 mmol), and $Mg(OAc)_2{\cdot}4H_2O$ (157 mg, 0.73 mmol) in *i*-AmOH (12 mL) in the presence of DBU (0.5 mL) was heated to reflux under argon for 33 h. The reaction mixture was cooled to room temperature and the mixture MeOH:H_2O (1:1 V/V) was added. The blue precipitate was filtered and washed by water and MeOH. The target compound **6b** (16 mg, 22.2%) was separated using gel permeation chromatography (C_6H_6:pyridine (100:1)). ^1H NMR (400.13 MHz, Py-d_5+1 eq of ethylene glycol, 20 °C): δ = 0.85 (t, $J_{H,H}$ = 7.34 Hz, 12H, CH_3); 0.87 (t, $J_{H,H}$ = 7.34 Hz, 12 H, CH_3); 0.88 (t, $J_{H,H}$ = 7.34 Hz, 12 H, CH_3); 1.30 (m, $J_{H,H}$ = 7.34, 3.20, Hz, 24 H, CH_2); 1.49 (tt, $J_{H,H}$ = 7.34, 3.20 Hz, 24H, CH_2); 2.67 (t, $J_{H,H}$ = 7.34 Hz, 24 H); 7.89 (with pyridine residual protons, 12H, H_{Ar}) 9.68 (br s, 4 H, H_{Nph}). MS (MALDI-TOF), *m*/*z*: 1718 $[M]^+$. UV/Vis (THF) λ_{max}/nm: 360; 709; 751; 800.

2.3. Synthesis of metal-free binuclear phthalocyanines

2.3.1. Bis(9(10)²,14(15)²,19(20)²-tri-tert-butyltribenzo [i,n,s]-7,12,17,22-tetraazaporphyrino)[b,g] naphthalene ***7a***

The binuclear phthalocyanine **6a** (40 mg, 0.030 mmol) was dissolved in concentrated sulfuric acid (4 mL). This solution was poured into the ice. At the same time the green precipitate was formed. This precipitate was filtered and washed by MeOH to give **7a** (38 mg, 99%). MS (MALDI-TOF), *m*/*z*: 1338 $[M]^+$. UV/Vis (TCB) λ_{max}/nm: 348; 700; 725; 764; 802. IR (KBr): ν_{max}/cm^{-1} 1512, 1599 ($\nu_{C=N}$); 937–1296 (ν_{C-H}).

2.3.2. Bis(9²,10²,14²,15²,19²,20²-hexa-butyltribenzo [i,n,s]-7,12,17,22-tetraazaporphyrino)[b,g] naphthalene ***7b***

The binuclear phthalocyanine **6b** (56 mg, 0.030 mmol) was dissolved in concentrated sulfuric acid (5 mL). This solution was poured into the ice. At the same time the green precipitate was formed. This precipitate was filtered and washed by MeOH to give **7b** (54 mg, 99%). ^1H NMR (400.13 MHz, Py-d_5, 20 °C): δ = 0.58–1.12 (m, 3H, CH_3); 1.15–1.50 (m, 4H, CH_2); 2.72 (m, 2H, CH_2). MS (MALDI-TOF), *m*/*z*: 1674 $[M]^+$. UV/Vis (THF) λ_{max}/nm: 335; 693; 721.

2.4. Synthesis of binuclear phthalocyanine complexes of the REE and Ni

2.4.1. General procedure

The metallation of binuclear phthalocyanine ligands **7** (0.004 mmol) was realized by heating to reflux in *i*-AmOH (5 mL) for 2–3 min in the presence of $M(OAc)_m{\cdot}nH_2O$ (0.04 mmol, M = Lu (**10a** and **10d**), Er (**10b**), Gd (**10c**), Ni (**10e**)), and lithium methylate (2.0 mg, 53.00 mmol). The solvent was evaporated and the residue obtained was dissolved in THF. The insoluble admixtures of inorganic compounds were filtered. The evaporation of THF gave the corresponding compound **10** as dark-greenish powders.

2.4.2. (Bis(9(10)²,14(15)²,19(20)²-tri-tert-butyltribenzo [i,n,s]-7,12,17,22-tetraazaporphyrino)[b,g] naphthalene) dilutetium diacetate ***10a***

Yield 7.0 mg (98%). MS (MALDI-TOF), *m*/*z*: 1936 $[M-2OAc+2HY]^+$, 1338 $[M-2Lu+4H-2OAc]^+$. UV/Vis (THF) λ_{max}/nm: 350; 704; 749; 791.

2.4.3. (Bis(9(10)²,14(15)²,19(20)²-tri-tert-butyltribenzo [i,n,s]-7,12,17,22-tetraazaporphyrino)[b,g] naphthalene) dierbium diacetate ***10b***

Yield 6.7 mg (90%). MS (MALDI-TOF), *m*/*z*: 1975 $[M-2OAc+2HY]^+$, 1679 $[M-21Me-2OAc+2HY]^+$. UV/Vis (THF) λ_{max}/nm: 355; 703; 749; 790.

2.4.4. (Bis(9(10)²,14(15)²,19(20)²-tri-tert-butyltribenzo [i,n,s]-7,12,17,22-tetraazaporphyrino)[b,g] naphthalene) digadolinium diacetate ***10c***

Yield 6.0 mg (94%). MS (MALDI-TOF), *m*/*z*: 2675 2·$[M-2Gd+4H-2OAc]^+$, 1935 $[M-2OAc+2HY]^+$, 1338 $[M-2Gd+4H-2OAc]^+$. UV/Vis (THF) λ_{max}/nm: 350; 702; 751; 790.

2.4.5. (Bis(9²,10²,14²,15²,19²,20²-hexa-butyltribenzo [i,n,s]-7,12,17,22-tetraazaporphyrino)[b,g] dilutetium diacetate ***10d***

Yield 8.5 mg (97%). MS (MALDI-TOF), *m*/*z*: 1684 $[M-6Bu-2OAc]^+$. UV/Vis (THF) λ_{max}/nm: 353; 707; 759; 803.

2.4.6. (Bis(9(10)²,14(15)²,19(20)²-tri-tert-butyltribenzo [i,n,s]-7,12,17,22-tetraazaporphyrino)[b,g] naphthalene) dinickel ***10e***

Yield 5.7 mg (98%). MS (MALDI-TOF), *m*/*z*: 1450 $[M]^+$, 2900 2·$[M]^+$, 4351 3·$[M]^+$, 5804 4·$[M]^+$. UV/Vis (TCB) λ_{max}/nm: 332, 707, 753, 796.

3. Results and discussion

3.1. Synthesis of binuclear phthalocyanines

The statistical condensation between bis(diiminoisoindoline) derivative and corresponding alkyl-substituted phthalonitriles was chosen for synthesis of planar binuclear phthalocyanines sharing a common naphthalene ring. The possibility of increasing yields of target compounds due to the simplicity of the synthetic procedure is an important advantage of this method in comparison with the reaction using the unsymmetrical substituted phthalocyanines [7]. Moreover, it is possible to carry out the experiment under mild conditions in contrast to the solid phase method [13].

Bis(diiminoisoindoline) derivative forming the naphthalene bridge was obtained according to Scheme 1.

Free radical bromination of 4,5-dibromo-*o*-xylene **1** under UV-irradiation conditions gave compound **2**. Further treatment with NaI eliminated bromine gave an intermediate *o*-quinodimethane derivative, which was intercepted by a Diels-Alder reaction with fumaronitrile and produced compound **3**. Compound **4** was obtained by cyanation of **3** under Rosenmund-von Braun conditions. This synthetic approach is the most preferable for **4**, because the standard method described in Ref. [14] led to a low yield of **4** (the authors [14] used 4,5-dimethyl-phthalonitrile as a starting compound). The reproduction of this literature route showed that bromination of 4,5-dimethyl-phthalonitrile gave less brominated products which were difficult to separate. So the target compound was obtained with a low yield (33%) [14] and the authors could not give the exact characteristics of the compound synthesized. The approach used in the present paper allowed the yield of **4** to be increased to 68%.

To increase the reactivity in phthalocyanine synthesis, tetranitrile **4** was converted to bis(diiminoisoindoline) derivative **5** by

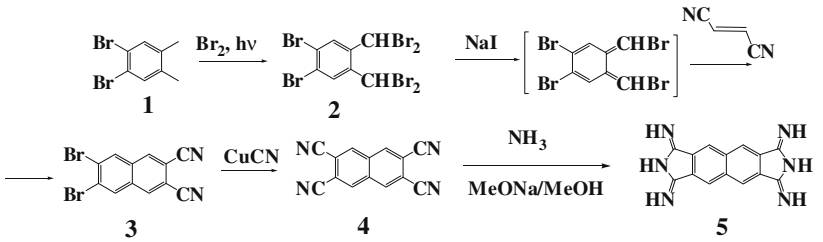

Scheme 1. Synthesis of bis(diiminoisoindoline) derivative **5**.

analogy with the published procedure for synthesis of bis(1,3-diiminoisoindoline) [8,15].

Template assembling of magnesium complexes and their further demetallation gave the metal-free phthalocyanines (Scheme 2).

The magnesium complexes **6** were synthesized by statistical condensation in boiling solvent under argon. The formation of symmetrical substituted phthalocyanine as by-products was found, which is typical for these types of reactions [6,15].

When using DMAE mentioned in the literature [5] as a solvent and a ratio of **5**: 4-*tert*-butylphthalonitrile (1:5), the low yield of **6a** was caused by incomplete cyclization (Scheme 3). To favour formation of **6a** by completing cyclization of the second ring at **8**, the ratio of initial compounds was changed to 1:20 although the product yield was not increased significantly (Table 1).)

Further optimization of reaction conditions has shown that employment of isoamyl alcohol–DBU system leads to the highest yield of **6a**, while trinuclear phthalocyanine **9** was obtained as a by-product (Scheme 3).

To avoid the formation of an isomers mixture (of which the highest possible quantity in the case of *tert*-butyl-substituted planar binuclear phthalocyanines can be 36), for ease of interpretation of NMR spectra, a magnesium complex **6b** was synthesized starting from 4,5-dibutylphthalonitrile (Scheme 2).

The metal-free binuclear phthalocyanines **7** were obtained upon treatment of magnesium complexes **6** with concentrated sulphuric acid using a standard technique [16]. Subsequent metallation of **7a** by REE and nickel acetates produced a series of complexes **10** in almost quantitative yields (Scheme 4). Dodeca-*n*-butyl-substituted binuclear phthalocyanine lutetium complex **10d** was synthesized by analogy with Scheme 4.

The binuclear phthalocyanines **10a**–**10d** bear the extra-ligands and consequently may exist in both *syn* and *anti* isomeric forms, which however cannot be separated using chromatographic methods [17].

3.2. Spectral properties of binuclear phthalocyanines

In Refs. [6,18] it was mentioned that planar binuclear phthalocyanines sharing a common benzene ring have a tendency to aggregation in non-coordinating solvents. In the case of the magnesium complexes **6**, broadening of the Soret (B) band and the Q-band (700–850 nm) and also a significant fall in the Q-band intensity were observed in non-coordinating solvents ($CHCl_3$, C_6H_6). The increase in solvent polarity improves spectrum resolution. Thus, in DMSO, pyridine, and THF an intensive absorption maximum was observed in the near IR-region, and the Soret band became sharp.

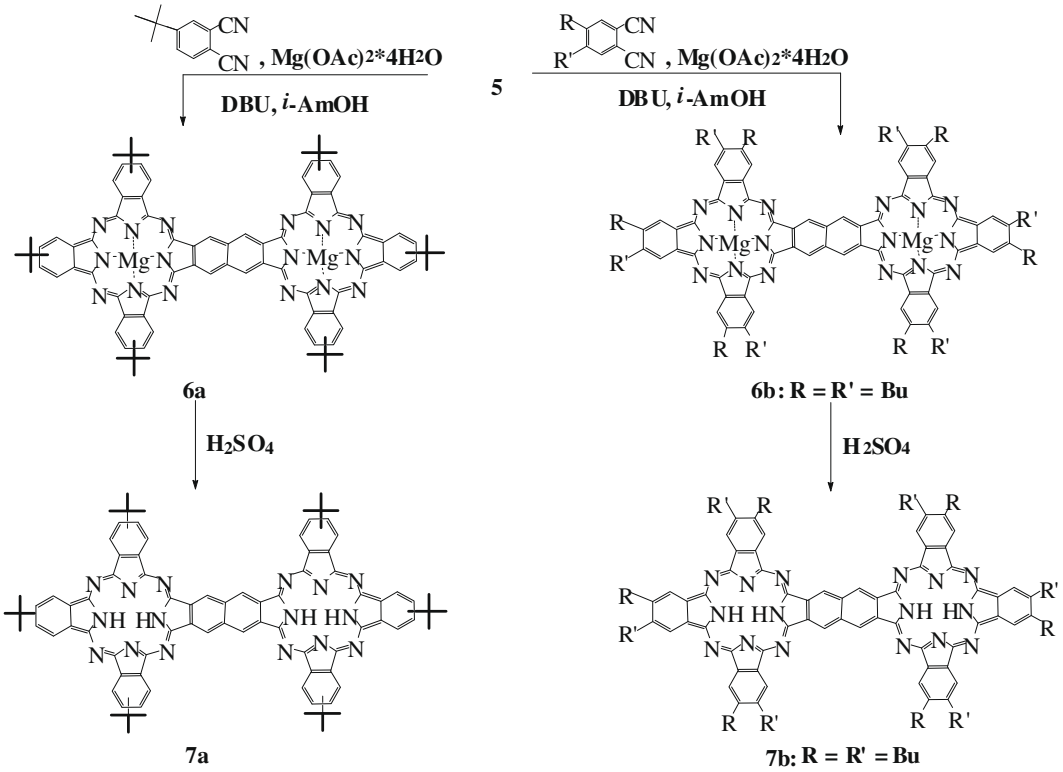

Scheme 2. Synthesis of binuclear phthalocyanine magnesium complexes and metal-free binuclear phthalocyanines.

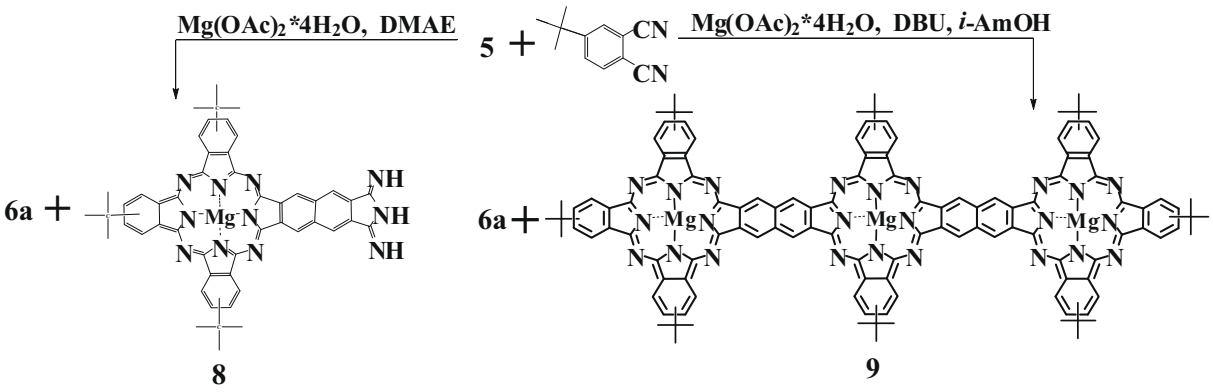

Scheme 3. Formation of complexes **8** and **9**.

Table 1
Synthetic conditions for compound **6a**.

Solvent/base	Ratio **5**: 4-*tert*-butylphthalonitrile	Time of reaction (h)	Yield (%)
DMAE	1:5	61	2
	1:20	17	6
i-AmOH/DBU	1:20	8	19.5

These changes can be explained by extra-coordination of solvent molecules to the magnesium ion, which prevents π-stacking interaction between binuclear phthalocyanine molecules in solution suppressing the aggregation. The typical changes in UV/Vis spectra are shown in Fig. 1 on an example of **6a**.

When comparing the spectra of *tert*-butyl-substituted (**6a**) and butyl-substituted (**6b**) magnesium complexes, 2 and 11 nm red shifts going from **6a** to **6b** were observed (Table 2) for the B- and Q-bands respectively. In comparison with binuclear magnesium complexes, an additional extension of the π-electron system for trinuclear phthalocyanine **9** gives a larger bathochromic shift of the Q-band.

It was determined that compound **6a** (THF) conformed to Beer's law for concentrations less than 10^{-5} M with the extinction coefficient of 3.3×10^5 M^{-1} cm^{-1} (λ = 789 nm). This value is comparable with ones for monophthalocyanines [19] but by an order of magnitude greater than that for the planar binuclear phthalocyanines described in literature [17,20].

It is noteworthy that the structure of the UV/Vis spectrum of metal-free binuclear phthalocyanine becomes clear and has the best resolution in *o*-DCB (Fig. 2).

In the case of REE phthalocyanines **10** the character of the central metal did not influence the Q-band position, and this was also observed for monophthalocyanines but not for diphthalocyanines [16]. However, a noticeable red shift going from **10a** to **10d** was observed. This effect can be explained by strengthening of the donor properties of substituents.

By the example of UV/Vis spectra of binuclear phthalocyanine complexes of REE it was clearly shown that three main absorption bands were observed in the region 700–800 nm (Fig. 3). A less intensive absorption band in the near IR-region for REE complexes in comparison with magnesium complexes seems to be caused by stronger aggregation due to a high coordination number of REE.

In order to unambiguously interpret absorption bands in UV/Vis spectra, the fluorescence spectra were investigated for compounds **6a** (Fig. 4) and **7a**.

In the case of **6a** THF solution (Fig. 5), the Stoke shift was not observed for the absorption band at λ = 709 nm. The Stoke shift of the absorption band at λ = 789 nm was 11 nm. Thus, due to the fluorescence spectra, these bands can be attributed to Q-bands.

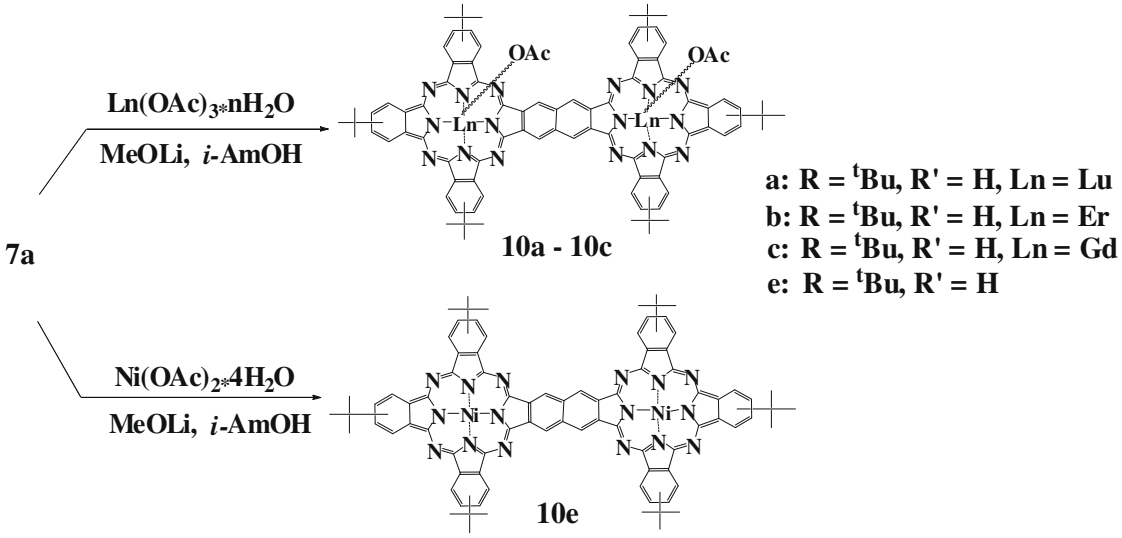

Scheme 4. Metallation of metal-free ligands **7a**.

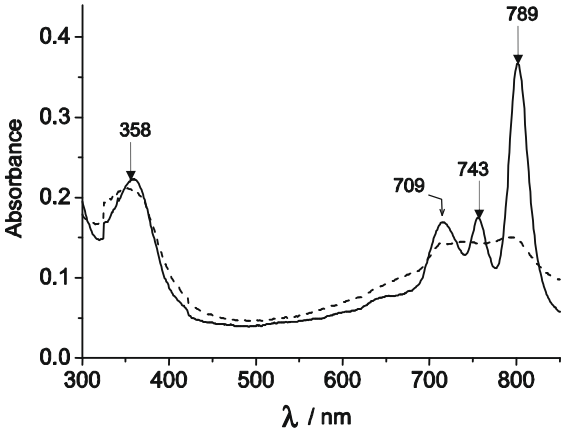

Fig. 1. UV/Vis spectra of **6a** in THF (solid line) and C_6H_6 (dashed line) (C = 2.27 μM).

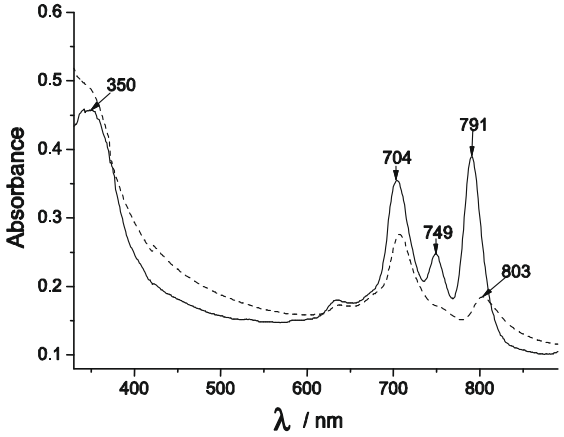

Fig. 3. UV/Vis spectra of **10a** (solid line) and **10d** (dashed line) in THF.

Table 2
Absorption bands of phthalocyanine complexes in THF.

Compound	λ (I/I_{max}), nm	Compound	λ (I/I_{max}), nm
6a	358(0.54); 709(0.42); 743(0.48); 789(1.00)	**10a**	350(1.00); 704(0.78); 749(0.54); 791(0.85)
6b	360(0.94); 709(0.83); 751(0.55); 800(1.00)	**10b**	355(1.00); 703(0.90); 749(0.39); 790(0.53)
9	356(1.00); 809(0.71); 832(0.56); 855(0.54)	**10c**	350(1.00); 702(0.97); 748(0.48); 790(0.32)
		10d	353(1.00); 707(0.57); 759(0.35); 803(0.38)

The absorption band at λ = 743 nm is reflected relative to the axis which passes across the intersection of the absorption and fluorescence spectra and was consequently attributed to a vibrational satellite.

In the case of metal-free binuclear phthalocyanine, the absorption bands at λ = 725 nm and λ = 802 nm were attributed to Q-bands and the absorption bands at λ = 700 nm and λ = 764 nm were attributed to vibrational satellites (Fig. 6). The Stoke shift was not observed in the case of the absorption band at λ = 725 nm; however the Stoke shift of the absorption band at λ = 802 nm was 14 nm.

The results obtained could be interpreted well with molecular orbital calculations for the planar binuclear phthalocyanines described in Ref. [8]. These data predict the splitting of the Q-band due to the independent nature of the two phthalocyanine rings. Moreover, in comparison with planar binuclear phthalocyanine sharing a common benzene ring, the hypsochromic shift of the Q-band is expected due to the increase in the HOMO–LUMO distance for planar binuclear phthalocyanine sharing a common naphthalene ring.

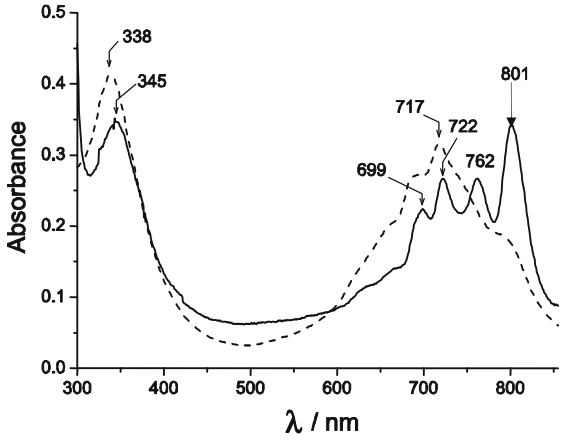

Fig. 2. UV/Vis spectra of **7a** in *o*-DCB (solid line) and in THF (dashed line).

3.3. ^{1}H NMR spectroscopy of planar binuclear phthalocyanine complexes

A number of problems accompany the NMR study of planar binuclear phthalocyanines. The authors of Ref. [17] note that ^{1}H NMR spectra of planar binuclear phthalocyanines sharing a common naphthalene ring are characterized by broad signals in the aromatic area. However, deep insight into the nature of this phenomenon is not discussed. Thus, it is very important to consider the influence of solvent nature and temperature on the character of ^{1}H NMR spectra in order to find optimum NMR conditions for these types of complexes.

When ^{1}H NMR spectra of the complexes are observed in non-coordinating solvents, only broad signals are observed, probably due to the aggregation phenomenon. Compounds bearing *tert*-butyl-substituents, which cause the signals of binuclear phthalocyanine complex isomers to be unequal, hinder the correlation of the spectrum in the aliphatic region, but compound **7b** possesses low solubility. Due to the mentioned restrictions, we chose compound **6b** for detailed NMR investigation.

Preliminary investigation of the ^{1}H NMR spectrum of the *n*-butyl-substituted magnesium complex of binuclear phthalocyanine **6b** was carried out in pyridine-d_5. However, even in highly polar pyridine, solvent signals of aromatic protons H_{Ar} were not observed due to the aggregation of the phthalocyanine. This can be explained by strong π-stacking interactions between phthalocyanine molecules in solution. In order to examine this hypothesis several experiments at elevated temperature were carried out. The values of T_2 are diminished by the temperature rise (see Table 1 in Supplementary material), which supports the hypothesis of the aggregation of the phthalocyanine moiety. This observation correlates well with previous findings. A crucial increase in spectra resolution was achieved by the addition of a drop of ethylene glycol, a good coordination molecule for the oxophilic magnesium cation. The tertiary complex formation between magnesium, phthalocyanine, and ethylene glycol was confirmed by DOSY experiment (Fig. 7). Almost the same diffusion coefficient for phthalocyanine **6b** and coordinated ethylene glycol supports the tertiary complex formation. Moreover, the complex showed a clear

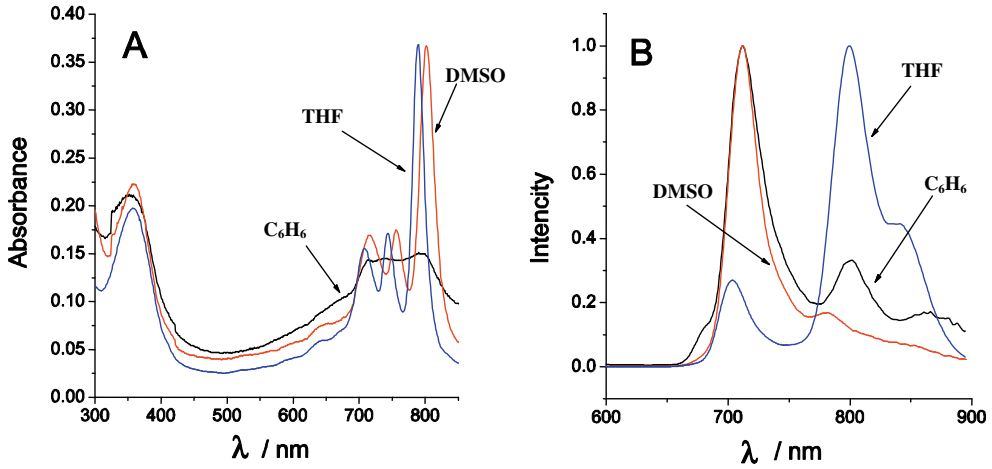

Fig. 4. UV/Vis (A) and fluorescence spectra (B) (λ_{ex} = 355 nm) of **6a** (C = 2.20 μM)

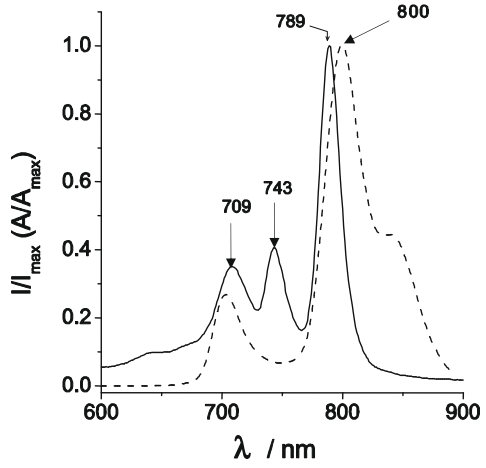

Fig. 5. UV/Vis (solid line) and fluorescence (dashed line) spectra (λ_{ex} = 355 nm) of **6a** in THF (C = 2.20 μM).

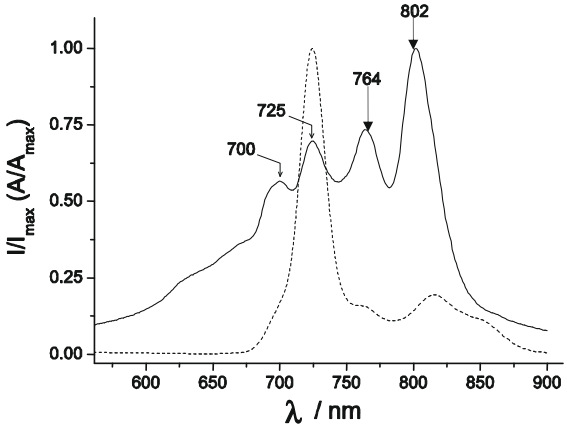

Fig. 6. UV/Vis (solid line) and fluorescence (dashed line) spectra (λ_{ex} = 355 nm) of **7a** in *o*-DCB.

NMR spectrum for phthalocyanine moiety and T_2 values for all of the aliphatic protons were diminished to a magnitude of about 1.8 Hz. These clearly show that the broadening of the signals originally observed originated from the molecules approaching aggregation, which is eliminated by coordination of extra-ligands to the metal ion.

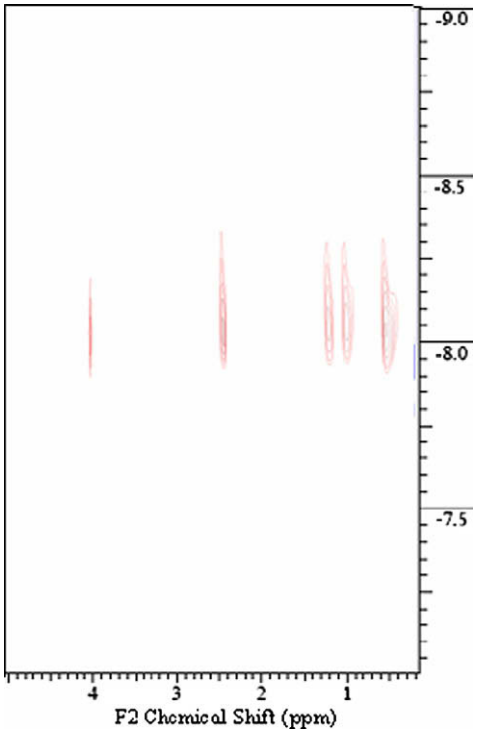

Fig. 7. DOSY-spectrum of phthalocyanine **6b** in the presence of ethylene glycol.

3.4. Electrochemistry

3.4.1. Cyclic voltammetry

The redox proprieties of phthalocyanines were studied using cyclic voltammetry (CV) on a platinum electrode. DCB was chosen as a solvent due to the good solubility of the binuclear phthalocyanines and the great convenience of this solvent for electrochemical measurements according to our previous experience. Fig. 8 shows cyclic voltammograms of **6a**, **6b**, and *t*BuPcMg (as a monophthalocyanine control) with the half-wave potentials of redox couples listed in Table 3. *t*BuPcMg gave three quasi-reversible redox-processes (ΔE_p < 0.15 V, $i_{p,a} = i_{p,c}$, $i_p \sim v^{0.5}$) at potentials which are in good agreement with previously published data for *t*BuPcCu [21]. Compound **6a** showed a slight anodic shift of the potential of red_1 and the same value of red_2 compared with the potentials of couples for monophthalocyanine. CV of **6b** revealed a splitting of

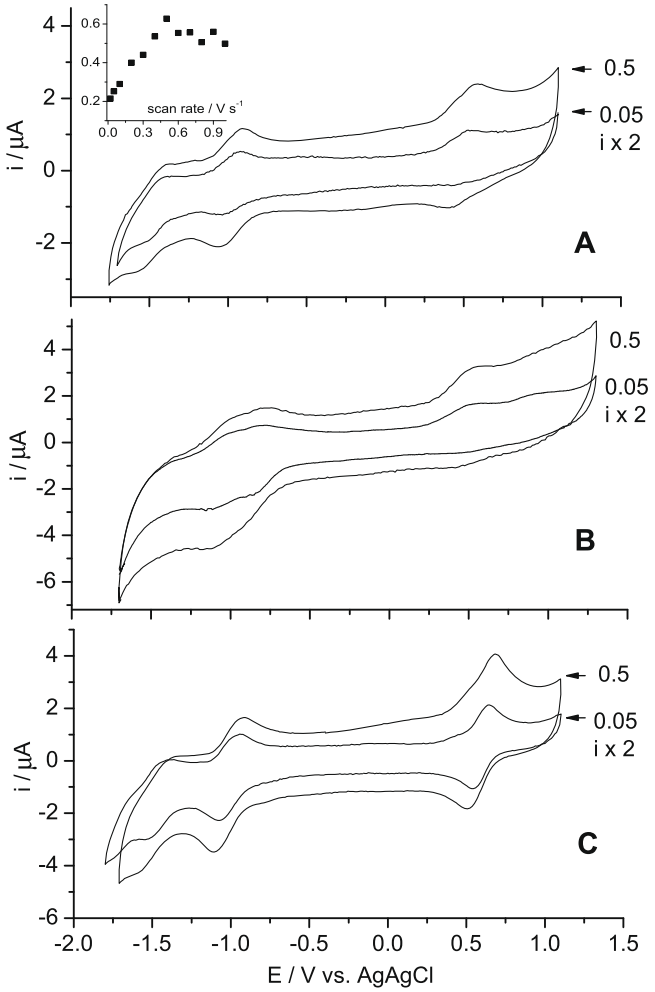

Fig. 8. Cyclic voltammograms for **6a** (A), **6b** (B), and *t*BuPcMg (C) in DCB. The numbers near the curves denote scan rates in V s^{-1}; the currents for 0.05 V s^{-1} were multiplied by 2 for scaling. The insert shows the dependence of the ratio between peaks of current in the direct and back scans on the scan rate for the oxidation process of **6a**.

Table 3
Half-wave potentials for phthalocyanines derivatives in DCB.[a]

Phthalocyanine	$E_{1/2}$ (red_2)/V	$E_{1/2}$ (red_1)/V	$E_{1/2}$ (ox_1)/V
*t*BuPcMg	−1.45 (−2.08)	−1.02 (−1.65)	0.60 (−0.03)
*t*BuPc$_2$Mg$_2$ (**6a**)	−1.46 (−2.09)	−0.98 (−1.61)	0.49 (−0.14)
BuPc$_2$Mg$_2$ (**6b**)	–	−0.97 (−1.60)[b]	0.49 (−0.14)[c]

[a] Values with respect to Fc^+/Fc couple are given in brackets.
[b] Mean potential of the splitting with ΔE_{split} = 0.19 V.
[c] An additional irreversible redox-process with $E_{1/2}$ = 0.96 V was observed.

the couple red_1 with ΔE_{split} = 0.19 V and a middle value of the potentials almost equal to the potential of red_1 for **6a**. However, the couple red_2 of **6b** was missing, probably because it was outside the voltage range.

In contrast to monophthalocyanines, only an irreversible redox wave of ox_1 appeared for binuclear phthalocyanines at the potential of 0.49 V that is, 0.11 V less positive than that for *t*BuPcMg. The cathodic peak on the back scan was much lower than the anodic peak on the direct scan, but the ratio between them increased with the scan rate and reached a value of 0.5–0.6 at the scan rate of 0.5 V s^{-1} (see inset in Fig. 8). Such electrochemical behaviour is probably due to coupling of the electrochemical process with simultaneous chemical reaction [22,23]. However, while the nature of this reaction is not clearly understood, aggregation between the oxidized form (as electron acceptor) and native form (as electron donor) seems to be the most probable process. Sandwich-like aggregates with an oxidized phthalocyanine in the middle can show a low rate of reduction on the back scan. High scan rates do not provide sufficient time for aggregates formation or reorganization, and thus the current of the peak increases on the back scan. Additional evidences of high ability to aggregation in DCB are (i) broadened Q-bands in the electronic spectrum of **6a** and (ii) deviation from Beer's law at concentrations above 7×10^{-6} M (data not shown).

Oxidation of **6b** was more irreversible compared with **6a**, and only a minor current was observed on the back scan even at high scan rates. This result is also in agreement with the assumption of aggregation as the chemical process, since Bu-substituted phthalocyanines with six butyl groups form aggregates more easily than *t*Bu-substituted ones, which have only four *tert*-butyl groups. As a feature of **6b**, an additional irreversible peak at a potential of 0.96 V was observed in the anodic area.

The previously described binuclear phthalocyanine sharing a common benzene ring gave a splitting of all redox couples with ΔE_{split} = 0.24 V. In the case of the naphthalene bridge, a smaller value is expected due to the increase in distance between monomer centres. In fact, only **6b** showed the splitting for one of the redox couples. The peak separation in the other cases is probably not sufficient to be resolved in CV. However, the splitting of **6b** could also arise due to a strong π-stacking interaction because of aggregation [24,25]. As a result, the approximate redox potentials and kinetic restrictions of back reduction from the oxidized state of the binuclear phthalocyanines were determined using CV experiments.

3.5. Spectroelectrochemistry

In order to obtain information on the thermodynamic reversibility of the oxidation and electrochromic properties of binuclear phthalocyanines, spectroelectrochemical investigation of **6a** was performed. Open circuit potentials and electronic spectra were measured during the electrolysis to relate an equilibrium potential to changes in the phthalocyanine. While two bands at λ = 709 and 800 nm decreased when oxidation was started (Fig. 9A), new bands at λ = 520 and 865 nm appeared according to the formation of a cation radical [16,26]. However, absorbance of the Q-band fell unevenly. The graph of dependence of the absorbance at λ = 709 and 800 nm on the potential is shown in Fig. 10. In the potential window between 0.2 and 0.45 V the absorbance at λ = 800 nm rapidly and reversibly changed. In contrast, the absorbance at λ = 709 nm mostly changed at potentials between 0.50 and 0.75 V. Thus, the spectroelectrochemical investigation has clearly revealed two stages of the oxidation of **6a**. A distance between the waves of the absorbance-potential curves (Fig. 10) was 0.20–0.25 V, which is close to the expected splitting of two one-electron oxidation steps for binuclear phthalocyanines [8]. Spectroelectrochemical study of the previously described binuclear phthalocyanine sharing common benzene ring [8] has not shown a two-stage drop in Q-bands, but independent changes have been noted in the band at λ = 865 nm, attributed to distortion of the planar structure of binuclear phthalocyanine. Thus, our studies have demonstrated, for the first time, two-stage changes in the Q-bands of binuclear phthalocyanine. In the back reduction from the totally oxidized form to the initial form, the complex was fully regenerated (Fig. 9B). This clearly demonstrates thermodynamic reversibility of the oxidation process of **6a**, whereas cyclic voltammetry showed sufficient kinetic restrictions of the back reduction.

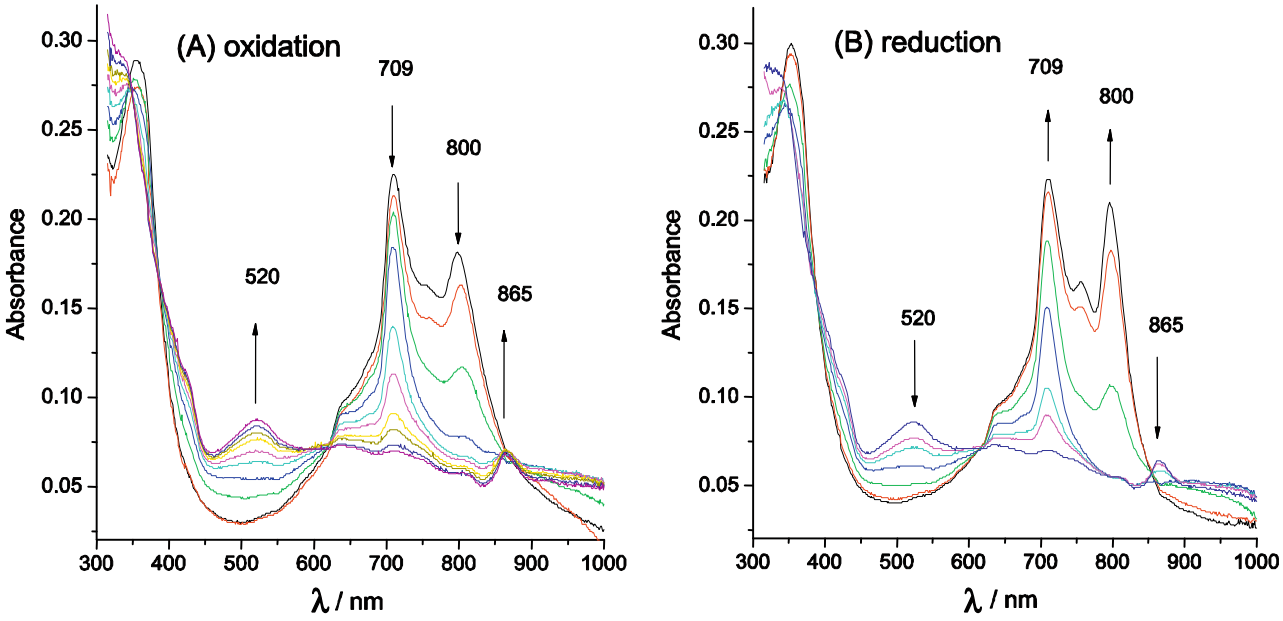

Fig. 9. Electronic spectra of **6a** obtained at different degrees of oxidation (A) and back reduction from the oxidized state (B). Equilibrium potentials of the working electrode (in V) from up to down (A): 0.2, 0.35, 0.41, 0.49, 0.61, 0.66, 0.68, 0.70, 0.73, 0.75; (B): 0.73, 0.69, 0.63, 0.50, 0.35, 0.26, 0.2.

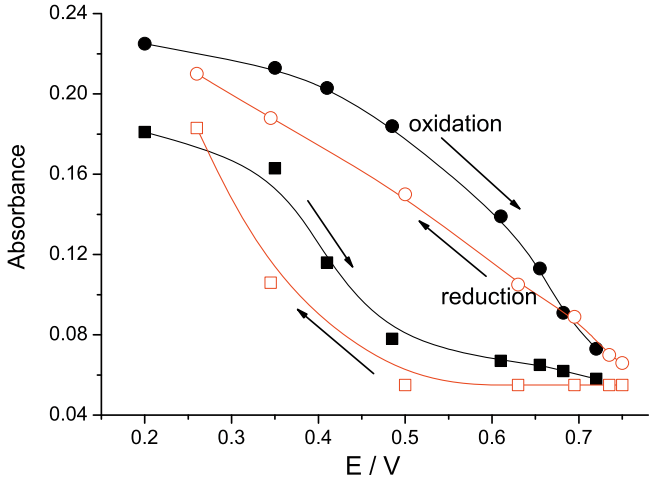

Fig. 10. Dependence of the absorbance at wavelengths of 709 nm (-●-, -○-) and 800 nm (-■-, -□-) calculated from Fig. 9 on the equilibrium potential of the working electrode in a solution of **6a**. The potential was measured in the oxidation (-●-, -■-) and reduction (-○-, -□-) directions.

4. Conclusion

In conclusion, we have presented a novel approach to planar binuclear phthalocyanines sharing common naphthalene ring. The described method is convenient and target compounds were obtained with high yields. Particularly, novel trinuclear phthalocyanine and unsymmetrical substituted phthalocyanine A_3B were synthesized and characterized. For all compounds obtained, the intensive absorption band in the near IR-region was found. The investigation of electrochemical and spectroelectrochemical properties of the planar binuclear phthalocyanines sharing a common naphthalene ring was reported for the first time. We believe that the features detected and the ease of synthesis open new perspectives for the use of polynuclear phthalocyanines in electronically controlled optical devices and memory storage devices.

Acknowledgements

This study was supported by the Russian Foundation for Basic Research (grant no. 08-0300753) and the programme of the Presidium of the Russian Academy of Science "Development of a strategy of organic synthesis and creation of compounds with valuable and applied proprieties".

Appendix A. Supplementary material

Supplementary data associated with this article can be found, in the online version, at doi:10.1016/j.ica.2010.02.011.

References

[1] M.J.F. Calvete, D. Dini, M. Hanack, J.C. Sancho-Garcia, W. Chen, W. Ji, J. Mol. Model. 12 (2006) 543.
[2] Z. Peng, X. Song, L. Zhong-Yu, Z. Fu-Shi, Chin. Phys. Lett. 2 (2008) 2058.
[3] L. Zhi, T. Gorelik, J. Wu, U. Kolb, K. Müllen, J. Am. Chem. Soc. 127 (2005) 12792.
[4] Y.J. Zhang, L.S. Li, J. Jin, S. Jiang, Y. Zhao, T.J. Li, Langmuir 15 (1999) 2183.
[5] J. Yang, M.R. Van De Mark, Tetrahedron Lett. 34 (1993) 5223.
[6] A.Y. Tolbin, V.E. Pushkarev, L.G. Tomilova, N.S. Zefirov, Russ. Chem. Bull. 55 (2006) 1155.
[7] M. Calvete, M. Hanack, Eur. J. Org. Chem. (2003) 2080.
[8] N. Kobayashi, H. Lam, W.A. Nevin, P. Janda, C.C. Leznoff, T. Koyama, A. Monden, H. Shirai, J. Am. Chem. Soc. 116 (1994) 879.
[9] S. Makarov, A.V. Piskunov, O.N. Suvorova, G. Schnurpfeil, G.A. Domrachev, D. Wöhrle, Chem. Eur. J. 13 (2007) 3227.
[10] V.E. Pushkarev, A.V. Ivanov, I.V. Zhukov, E.V. Shulishov, Y.V. Tomilov, Russ. Chem. Bull. (2004) 554.
[11] S.A. Mikhalenko, S.V. Barkanova, O.L. Lebedev, E.A. Luk'yanets, Zh. Obshch. Khim. 41 (1971) 2735 (in Russian).
[12] W. Freyer, L.Q. Minh, J. Prakt. Chem. 329 (1987) 365.
[13] A.Y. Maksimov, A.V. Ivanov, Y.N. Blikova, L.G. Tomilova, N.S. Zefirov, Mendeleev Commun. (2003) 70.
[14] E.I. Kovshev, E.A. Luk'yanets, J. All-Union Chem. Soc. (1975) 231 (in Russian).
[15] S. Makarov, C. Litwinski, E.A. Ermilov, O. Suvorova, B. Röder, D. Wöhrle, Chem. Eur. J. 12 (2006) 1468.
[16] T.V. Dubinina, R.A. Piskovoi, A.Yu. Tolbin, V.E. Pushkarev, M.Yu. Vagin, L.G. Tomilova, N.S. Zefirov, Russ. Chem. Bull. 57 (2008) 1912.
[17] M.J.F. Calvete, D. Dini, S.R. Flom, M. Hanack, R.G.S. Pong, J.S. Shirk, Eur. J. Org. Chem. (2005) 3499.
[18] G. Torre, M.V. Martinez-Diaz, T. Torres, J. Porphyr. Phthalocyan. 3 (1999) 560.

[19] M. Brewis, M. Helliwell, N.B. McKeown, Tetrahedron 59 (2003) 3863.
[20] N. Kobayashi, H. Ogata, Eur. J. Inorg. Chem. (2004) 906.
[21] N. Kobayashi, S. Nakajima, H. Ogata, T. Fukuda, Chem. Eur. J. 10 (2004) 6294.
[22] A.J. Bard, L.R. Faulkner, in: Electrochemical Methods: Fundamentals and Applications, second ed., John Wiley and Sons, Inc., 2001, pp. 496–500.
[23] J. Heinze, Angew. Chem., Int. Ed. 23 (1984) 831.
[24] H. Isago, C.C. Leznoff, M.F. Ryan, R.A. Metcalfe, R. Davids, A.B.P. Lever, Bull. Chem. Soc. Jpn. 71 (1998) 1039.
[25] M. Morisue, K. Kameyama, Y. Kobuke, Bull. Chem. Soc. Jpn. 82 (2009) 574.
[26] N. Kobayashi, Coord. Chem. Rev. 227 (2002) 129.